Journal of Innovative Optical Health Sciences
Vol. 11, No. 4 (2018) 1850020 (9 pages)

DOI: 10.1142/S1793545818500207

Degradation of multiphoton signal and resolution when focusing through a planar interface with index mismatch: Analytical approximation and numerical investigation

Ping Qiu*,‡ and Chen He†
*College of Physics and Energy, Shenzhen University
Shenzhen, Guangdong 518060, P. R. China
†Key Laboratory of Optoelectronic Devices and
Systems of Ministry of Education and Guangdong Province
College of Optoelectronic Engineering, Shenzhen University
Shenzhen, Guangdong 518060, P. R. China
‡pingqiu@szu.edu.cn

Received 3 March 2018
Accepted 16 April 2018
Published 9 May 2018

Multiphoton microscopy (MPM) is an invaluable tool for visualizing subcellular structures in biomedical and life sciences. High-numerical-aperture (NA) immersion objective lenses are used to deliver excitation light to focus inside the biological tissue. The refractive index of tissue is commonly different from that of the immersion medium, which introduces spherical aberration, leading to signal and resolution degradation as imaging depth increases. However, the explicit dependence of this index mismatch-induced aberration on the involved physical parameters is not clear, especially its dependence on index mismatch. Here, from the vectorial equations for focusing through a planar interface between materials of mismatched refractive indices, we derive an approximate analytical expression for the spherical aberration. The analytical expression explicitly reveals the dependence of spherical aberration on index mismatch, imaging depth and excitation wavelength, from which we can expect the following qualitative behaviors: (1) Multiphoton signal and resolution degradation is less for longer excitation wavelength, (2) a longer wavelength tolerates a higher index mismatch, (3) a longer wavelength tolerates a larger imaging depth and (4) both signal and resolution degradations show the same dependence on imaging depth, regardless of NA or immersion on the condition that the integration angle is the same. Detailed numerical simulation results agree quite well with the above expectations based on the analytical approximation. These theoretical results suggest the use of long excitation wavelength

‡Corresponding author.

to better suppress index mismatch-induced signal and resolution degradation in deep-tissue MPM.

Keywords: Biomedical optical imaging; nonlinear optics; optical microscopy.

1. Introduction

Since its demonstration in 1990,[1] multiphoton microscopy (MPM) has advanced in both fundamental theories and technologies. The intrinsic 3D sectioning capability, deep-tissue penetration, subcellular resolution and functional imaging capability make it ideal for a variety of applications in neuroscience,[2] oncology[3] and many others in biomedical and life sciences. A variety of MPM modalities have been experimentally demonstrated, covering nonlinear optical effects of various orders. In terms of multiphoton fluorescence, two-photon,[1,4] three-photon,[5–7] four-photon[8,9] and even five-photon fluorescence[6] generations have all been demonstrated, while in terms of the label-free harmonic generation imaging, second-harmonic,[10] third-harmonic[5,11] and even fourth-harmonic generation[6] imagings have all been demonstrated. So far, the mostly adopted imaging modality is two-photon fluorescence imaging. The emerging three-photon fluorescence imaging,[5,6] however, enables deeper penetration than the previously demonstrated two-photon fluorescence imaging and is especially useful for *in vivo* deep-tissue imaging.

Near-infrared (NIR) excitation light is almost exclusively used in MPM to reduce tissue scattering in order to achieve deep-tissue imaging. The 800-nm excitation window covered by the Ti:Sa mode-locked laser has been the main workhorse for MPM. With the development of ultrafast laser technology, it has been demonstrated that the 1300-nm window, enabled by optical parametric oscillators[12] and even amplifiers,[13] and the 1700-nm window, enabled by soliton self-frequency shift in photonic-crystal rods,[5,6] could facilitate even deeper penetration. Among these three excitation windows, 1700-nm window has been demonstrated to achieve the largest imaging depth.

In MPM, high-numerical-aperture (NA) immersion objective lenses are commonly used to get both subcellular resolution and high epi-collection efficiency. For deep-tissue imaging, there is another requirement on the objective lens, i.e., long working distance to guarantee physical access of the focus deep into tissues. Regarding immersion medium selection especially for long-working-distance objective lenses, there are two requirements: (1) The absorption has to be kept low to ensure sufficient excitation light is delivered through the immersion medium onto the sample.[14,15] (2) The refractive index has to be as close to that of the sample as possible. The index mismatch between the immersion medium and the sample will result in spherical aberration,[16] which degrades both multiphoton signal level and spatial resolution as imaging depth increases.[16,17]

The refractive index is highly varying among numerous biological tissues.[18,19] The immersion media are quite limited with discrete refractive indices including 1.33 for water, 1.4 for silicone oil and 1.52 for most other immersion oils (termed regular oil in this paper). Consequently, it is almost certain that there exists index mismatch between the immersion medium and biological tissues, and a resultant spherical aberration when doing MPM. The influence of this index mismatch-induced spherical aberration on MPM has been extensively investigated both experimentally and theoretically.[16,17,20] However, in view of the recently demonstrated MPM excited at longer excitation wavelengths, the following fundamental questions arise: What is the explicit dependence of the spherical aberration on the involving physical parameters? What is the impact of wavelength on this index mismatch-induced spherical aberration? Compared with shorter-wavelength excitation, is longer-wavelength excitation more tolerant or more susceptible to multiphoton signal and resolution degradation due to index mismatch?

It is our main aim here to answer the above questions. In the following sections, we first derive approximate analytical expression for the index mismatch-induced spherical aberration, from which we can explicitly obtain the quantitative dependence of spherical aberration on index mismatch, wavelength and imaging depth. Then we demonstrate detailed numerical simulation results, which agree quite well with the expectations based on analytical expression. Finally we reach the conclusion that

longer excitation wavelength is less susceptible to signal and resolution degradation compared with shorter wavelength.

2. Approximate Analytical Expression for Sphere Aberration

The model system in this paper is similar to those in Refs. 16 and 21. Basically, a high-NA objective lens focuses the excitation light from an immersion medium of refractive index n_1, through a planar interface, into a sample with uniform refractive index n_2. In this paper, the sample is assumed to be scattering- and absorption-free, to isolate the influence of index mismatch for investigation. This assumption also means that we do not consider the effect of reduced signal-to-background ratio (SBR) as imaging depth increases,[5] so we do not limit the simulated imaging depth to currently demonstrated values in experiments. In this section we will derive approximate analytical expression for the spherical aberration due to index mismatch to reveal the quantitative dependence on physical parameters.

When a plane wave linearly polarized along the x-axis is incident on the objective lens, the vectorial integral formula for the electric field of the excitation light near the focus in the sample, neglecting a constant common to all terms, is given by Ref. 21 in the cylindrical coordinate system (r, θ_p, z):

$$\begin{bmatrix} \mathbf{E}_x(r,\theta_p,z) \\ \mathbf{E}_y(r,\theta_p,z) \\ \mathbf{E}_z(r,\theta_p,z) \end{bmatrix} = \begin{bmatrix} I_0 + I_2\cos(2\theta_p) \\ I_2\sin(2\theta_p) \\ -2iI_1\cos\theta_p \end{bmatrix}, \quad (1)$$

where I_0, I_1 and I_2 are given by

$$\begin{aligned} I_0 &= \int_0^\alpha \sqrt{\cos\phi_1}(\sin\phi_1)(\tau_s + \tau_p\cos\phi_2)J_0(k_1 r\sin\phi_1) \\ &\quad \times \exp(i\Psi_{\text{sa}} + ik_2 z\cos\phi_2)d\phi_1, \\ I_1 &= \int_0^\alpha \sqrt{\cos\phi_1}(\sin\phi_1)\tau_p(\sin\phi_2)J_1(k_1 r\sin\phi_1) \\ &\quad \times \exp(i\Psi_{\text{sa}} + ik_2 z\cos\phi_2)d\phi_1, \\ I_2 &= \int_0^\alpha \sqrt{\cos\phi_1}(\sin\phi_1)(\tau_s - \tau_p\cos\phi_2)J_2(k_1 r\sin\phi_1) \\ &\quad \times \exp(i\Psi_{\text{sa}} + ik_2 z\cos\phi_2)d\phi_1. \end{aligned} \quad (2)$$

In the above equations, α is the maximum angle of integration given by $\sin\alpha = \text{NA}/n_1$. τ_s and τ_p are Fresnel coefficients for the s- and p-polarized lights, respectively. φ_2 is the refraction angle and is determined by φ_1. k_0, k_1 and k_2 are the wave vectors in vacuum, the immersion medium and the sample, respectively. The spherical aberration Ψ_{sa} is given by

$$\Psi_{\text{sa}}(\phi_1,\phi_2) = k_0 d(n_2\cos\phi_2 - n_1\cos\phi_1). \quad (3)$$

The interface is positioned at $-d$ from the Gaussian focus, so d represents the nominal imaging depth. It is clear that when the refractive indices are matched, i.e., $n_1 = n_2$, and as a result $\varphi_1 = \varphi_2$, Ψ_{sa} vanishes and no spherical aberration exists.

The two-photon and three-photon fluorescence signals are given by

$$\begin{aligned} S_2 &\propto [|\mathbf{E}|^2]^2|_{\max}, \\ S_3 &\propto [|\mathbf{E}|^2]^3|_{\max}. \end{aligned} \quad (4)$$

Spatial resolution is characterized as the full-width at half-maximums (FWHMs) of the point spread functions (PSFs) along the x-, y- and z-axes. Here we denote them as PSF_x, PSF_y and PSF_z, respectively.

Starting from Eq. (3), next we derive the approximate analytical expression for the spherical aberration to show the explicit dependence on index difference $\Delta n = n_2 - n_1$, wavelength and imaging depth:

$$\begin{aligned} \Psi_{\text{sa}} &= k_0 d[(n_1 + \Delta n)\cos\phi_2 - n_1\cos\phi_1] \\ &= k_0 d\left[n_1\left(1 + \frac{\Delta n}{n_1}\right)\sqrt{1 - \left(\frac{1}{1 + \frac{\Delta n}{n_1}}\right)^2\sin^2\phi_1}\right. \\ &\quad \left. - n_1\cos\phi_1\right]. \end{aligned} \quad (5)$$

Then we assume that the relative index mismatch $\Delta n/n_1 \ll 1$. This is a reasonable assumption. For example, the refractive index of the brain gray matter is 1.36. When using water immersion ($n_1 = 1.33$), $\Delta n/n_1 = 0.0226 \ll 1$. We expand the spherical aberration in series up to first order in $\Delta n/n_1$, yielding

$$\begin{aligned} \Psi_{\text{sa}} &= k_0 d\left(n_1\sqrt{1 - \sin^2\phi_1}\right. \\ &\quad \left. + n_1\frac{\frac{\Delta n}{n_1}}{\sqrt{1 - \sin^2\phi_1}} - n_1\cos\phi_1\right) \\ &= k_0 d\left(n_1\cos\phi_1 + \frac{\Delta n}{\cos\phi_1} - n_1\cos\phi_1\right) \\ &= \frac{2\pi d\Delta n}{\lambda\cos\phi_1}. \end{aligned} \quad (6)$$

Above Eq. (6) for the spherical aberration is the key expression in this paper, from which we can infer the following qualitative dependence of multiphoton signal and PSF degradation on the parameters of index difference Δn, wavelength λ and nominal imaging depth d:

(1) The spherical aberration is dependent on the excitation wavelength. The longer the excitation wavelength is, the larger is the spherical aberration. This statement also holds from the accurate expression for the spherical aberration, i.e., Eq. (3).
(2) The spherical aberration is proportional to the product of $\Delta n/\lambda$, which suggests that a longer excitation wavelength tolerates a larger index difference.
(3) The spherical aberration is proportional to the product of d/λ, which suggests that a longer excitation wavelength tolerates a larger imaging depth.
(4) The spherical aberration is proportional to Δn rather than n_1 or n_2, which suggests that for an immersion medium with different refractive index n_1, both the multiphoton signal and PSF dependences on imaging depth are the same, as long as the maximum angle of integration α remains the same.

3. Simulation Results and Discussion

To test the above expectations based on the approximate analytical expression [Eq. (6)], next we performed numerical simulations of Eqs. (1)–(4) to quantify the multiphoton signals as defined in Eq. (4). For fair comparison, the multiphoton signals and PSFs were normalized to those at the surface ($d = 0$). We calculated and compared the depth-dependent degradations of both multiphoton signals and PSFs, for different excitation wavelengths or refractive indices.

3.1. *Degradation versus excitation wavelength*

First we demonstrate the wavelength dependence of multiphoton signals and PSFs degradation. In our simulation we assumed NA = 1.05, $n_1 = 1.33$ (corresponding to water immersion) and $n_2 = 1.36$ for all excitation wavelengths. Figure 1 shows the depth dependence of two-photon and three-photon fluorescence signals, for excitation wavelengths of 850, 1300 and 1700 nm. It is clear that in the presence of index mismatch-induced spherical aberration, as imaging depth increases, both S_2 and S_3 will decrease, regardless of the excitation wavelength. For example, at an imaging depth of 1000 μm, S_2 and S_3 will drop to 1.9% and 0.25% of those at the surface ($d = 0$), respectively, for 850-nm excitation. The larger degradation of the three-photon signal compared with the two-photon signal is due to the higher-order nonlinearity and cubic dependence on intensity.

The most notable difference, when we compare the degradation behaviors of different excitation wavelengths, is that both S_2 and S_3 degrade less for longer excitation wavelength at the same imaging depth. For example, at $d = 1000\,\mu$m, S_2 and S_3 will

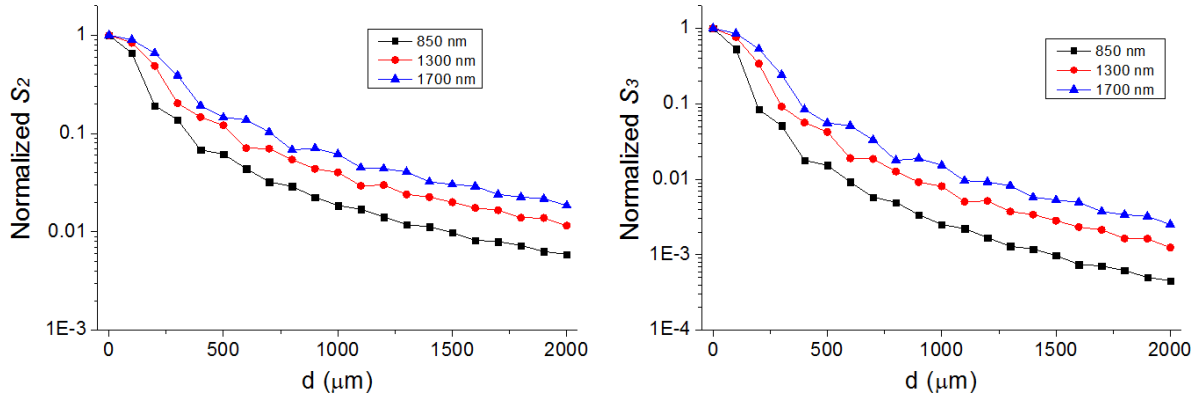

Fig. 1. Normalized (a) S_2 and (b) S_3 vs imaging depth for 850-nm, 1300-nm and 1700-nm excitations. S_2 and S_3 were normalized to those at the surface ($d = 0$). Also NA = 1.05, $n_1 = 1.33$ and $n_2 = 1.36$.

drop to 6.2% and 1.5% of those at the surface, respectively, with 1700-nm excitation, 3.3 times and 6 times higher than those with 850-nm excitation. So using longer excitation wavelength can help suppress the multiphoton signal degradation, due to the smaller spherical aberration it incurs compared with using shorter excitation wavelength. Among the three commonly used excitation windows, 1700-nm excitation suffers least from signal degradation due to spherical aberration.

We also calculated and compared the wavelength-dependent degradations of PSFs. Figure 2 show the two-photon PSF_x, PSF_y and PSF_z vs imaging depth, normalized to those at the surface, for 850-nm, 1300-nm and 1700-nm excitations. The degradation of resolution manifests itself as increasing PSFs when imaging deeper, as shown in Fig. 2. Unlike the monotonic decreasing of S_2 and S_3, all PSFs show some oscillation as imaging depth increases. The overall trend is that a longer excitation wavelength helps suppress resolution degradation, especially toward larger imaging depths. The three-photon PSFs (not shown) also show similar trends.

3.2. *Longer excitation wavelength tolerates high index mismatch*

Our analytical equation (6) reveals that the spherical aberration is proportional to $\Delta n/\lambda$, which suggests that a 2× increase in excitation wavelength and simultaneously a 2× increase in the index mismatch will result in the same spherical aberration. In this subsection we test this expectation through numerical simulation. In our simulation we assumed NA = 1.05 and $n_1 = 1.33$. The index mismatches $\Delta n = 0.03$ for 850-nm excitation and $\Delta n = 0.06$ for 1700-nm excitation, so that $\Delta n/\lambda$ remains the same for both excitation wavelengths. Figure 3 clearly shows that in spite of the different excitation wavelengths and index mismatches, the degradation of S_2 or S_3 on increasing the imaging depth is almost invariant for the same value of $\Delta n/\lambda$. For example, at an imaging depth of 2 mm, S_2 and S_3 will drop to 0.59% and 0.045% of those at the surface ($d = 0$), respectively, for 850-nm excitation. For comparison, these values are 0.61% and 0.047% for 1700-nm excitation, respectively. This means that with all other conditions being equal, a longer excitation wavelength is more tolerant of a larger index mismatch. The calculated degradation of PSFs also shows similar invariance on $\Delta n/\lambda$. For example, the calculated two-photon PSF_xs, PSF_ys and PSF_zs show highly overlapping degradation with imaging depth for both 850-nm and 1700-nm excitations, despite the oscillating behavior (Fig. 4).

3.3. *Longer excitation wavelength tolerates imaging depth*

From the analytical Eq. (6), we can also find that the spherical aberration is proportional to d/λ, which suggests that a 2× increase in excitation wavelength and simultaneously a 2× increase in the imaging depth will result in the same spherical aberration. Here we still assume NA = 1.05, $n_1 = 1.33$ and $n_2 = 1.36$ for both the 850-nm and 1700-nm excitations, the same as that in Sec. 3.1. We expect that the signal degradation will be the same for both

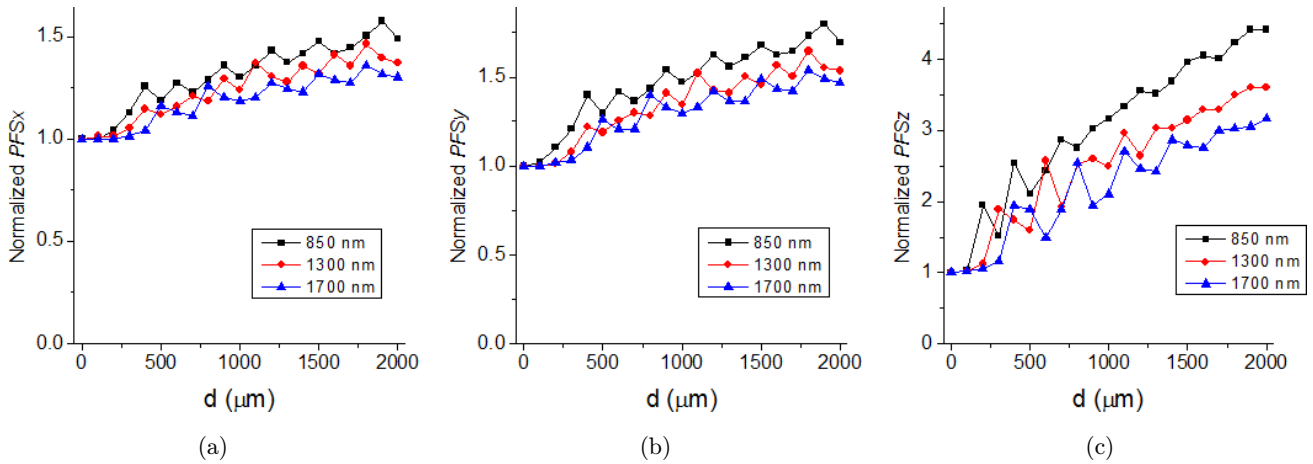

Fig. 2. Normalized two-photon (a) PSF_x, (b) PSF_y and (c) PSF_z vs imaging depth for 850-nm, 1300-nm and 1700-nm excitations. All PSFs were normalized to those at the surface ($d = 0$). Also NA = 1.05, $n_1 = 1.33$ and $n_2 = 1.36$.

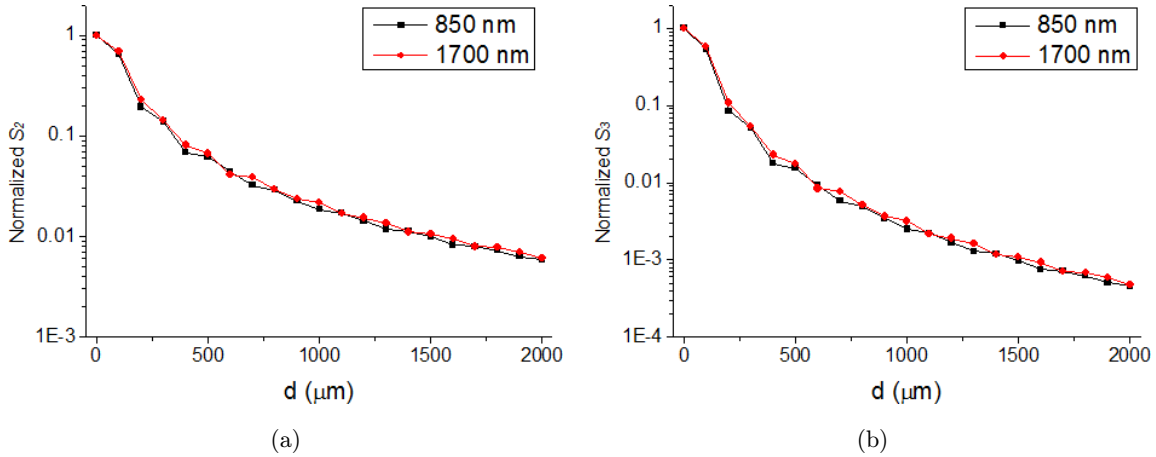

Fig. 3. (a) Normalized (a) S_2 and (b) S_3 vs imaging depth for 850-nm and 1700-nm excitations. S_2 and S_3 were normalized to those at the surface ($d = 0$). Also NA = 1.05 and $n_1 = 1.33$; $\Delta n = 0.03$ for 850-nm excitation and $\Delta n = 0.06$ for 1700-nm excitation.

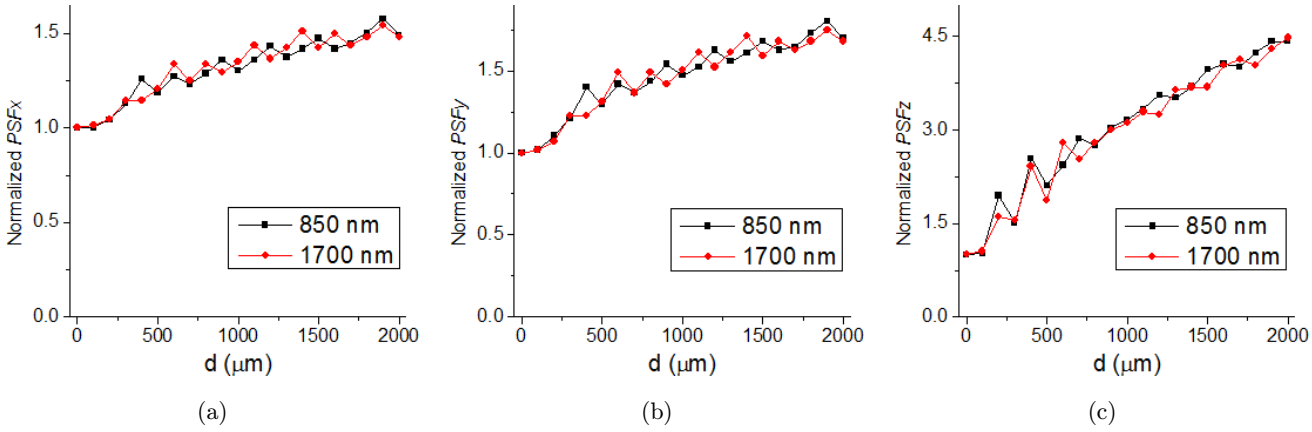

Fig. 4. Normalized two-photon (a) PSF_x, (b) PSF_y and (c) PSF_z vs imaging depth for 850-nm and 1700-nm excitations. All PSFs were normalized to those at the surface ($d = 0$). Also NA = 1.05 and $n_1 = 1.33$; $\Delta n = 0.03$ for 850-nm excitation and $\Delta n = 0.06$ for 1700-nm excitation.

wavelengths if $d/\lambda(1700\,\mathrm{nm}) = d/\lambda(850\,\mathrm{nm})$. This is indeed the case if we plot normalized signals using different abscissas for 850-nm and 1700-nm excitations, as shown in Fig. 5. With 1700-nm excitation, an imaging depth of 2000 μm leads to signal degradation similar to those with 850-nm excitation at an imaging depth of 1000 μm. The calculated normalized two-photon and three-photon PSFs vs imaging depth (not shown) also show the same tolerance of longer excitation wavelength for larger imaging depth.

3.4. *Dependency on index mismatch*

From Eq. (6) we can also find that for the same excitation wavelength, the spherical aberration is proportional to the index mismatch Δn, rather than the specific value of either n_1 or n_2. So we would expect that both the multiphoton signal and resolution degradations are not related to the specific immersion medium or the sample. In this subsection, we investigate the cases of three different immersion media and NAs: $n_1 = 1.33$ for NA = 1.05 (water immersion), $n_1 = 1.4$ for NA = 1.1 (silicone oil immersion) and $n_1 = 1.52$ for NA = 1.2 (regular oil immersion). The index mismatch $\Delta n = 0.06$ for all of these immersions. In order to maintain the total spherical aberration within the entire aperture determined by the objective lenses the same, the NAs were chosen such that α was the same for all the above three objective lenses. From Fig. 6 it can be clearly seen that using the same excitation

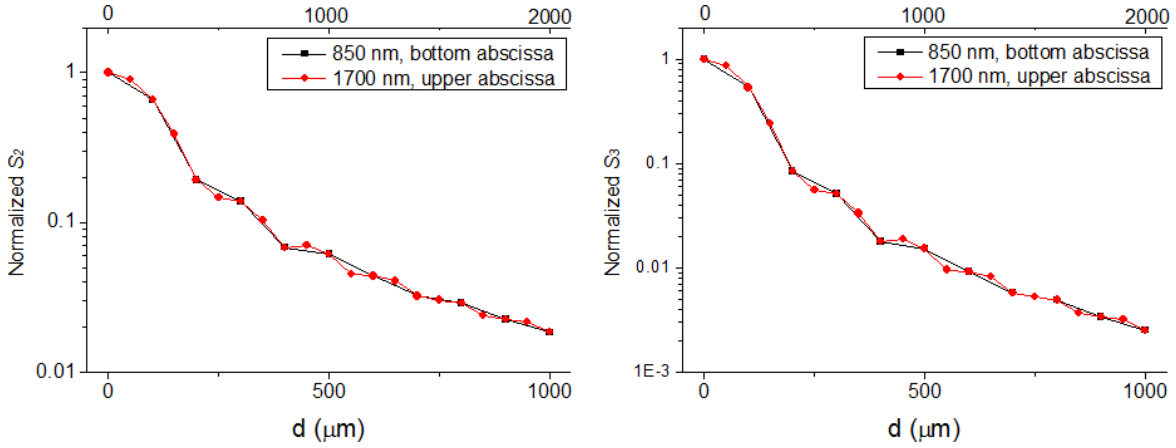

(a) (b)

Fig. 5. Normalized (a) S_2 and (b) S_3 vs imaging depth for 850-nm and 1700-nm excitations. S_2 and S_3 were normalized to those at the surface ($d = 0$). The abscissas are different for 850-nm (bottom abscissa) and 1700-nm (upper abscissa) excitation wavelengths. Also NA = 1.05, $n_1 = 1.33$ and $n_2 = 1.36$.

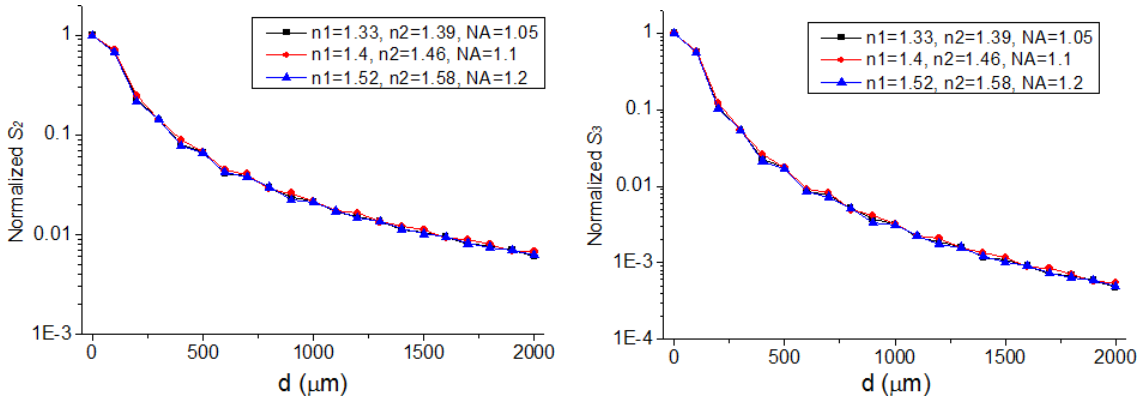

(a) (b)

Fig. 6. Normalized (a) S_2 and (b) S_3 vs imaging depth for 1700-nm excitation but with different immersion media and NAs. S_2 and S_3 were normalized to those at the surface ($d = 0$). Also $\Delta n = 0.06$. The n_1, n_2 and NA values are indicated in the figure.

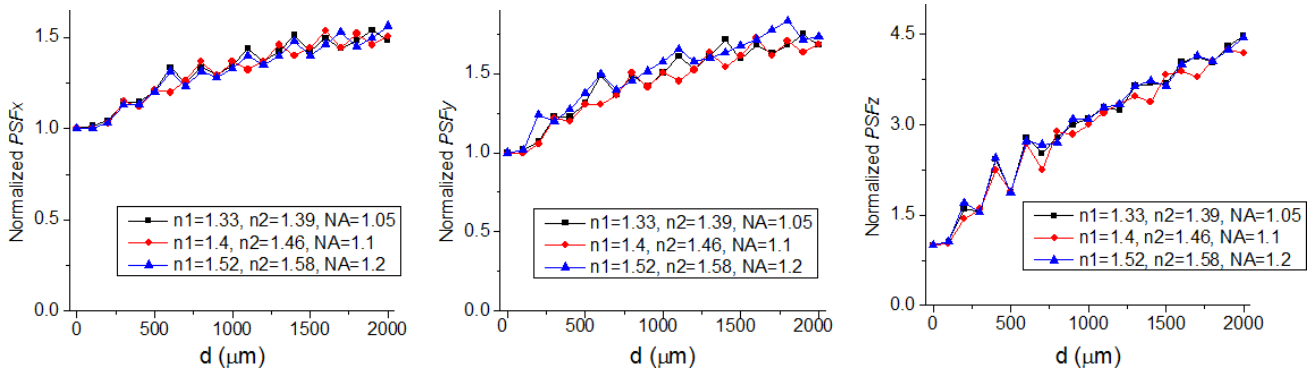

(a) (b) (c)

Fig. 7. Normalized two-photon (a) PSF_x, (b) PSF_y and (c) PSF_z vs imaging depth for 1700-nm excitation but with different immersion media and NAs. Also $\Delta n = 0.06$. The n_1, n_2 and NA values are indicated in the figure.

wavelength, the multiphoton signal degradation is almost the same as long as the index mismatch remains the same, regardless of the different immersion types or the sample refractive indices. As shown in Fig. 7, the calculated PSFs also show similar degradation trends upon increasing the imaging depth (taking two-photon PSFs for example), determined by the index mismatch.

4. Summary and Discussion

In order to understand the physical parameters that determine the spherical aberration when focusing through a planar interface with index mismatch, and their influence on the multiphoton signal and PSF degradation as imaging depth increases, in this paper, we derive an approximate analytical expression for the spherical aberration, clearly revealing its dependence on index mismatch, excitation wavelength and imaging depth. Detailed numerical simulation results agree quite well with our expectations from the analytical expression:

(1) Spherical aberration due to index mismatch is inversely proportional to wavelength. For the same imaging depth, longer excitation wavelength suffers from less spherical aberration-induced multiphoton signal and PSF degradation.
(2) A longer excitation wavelength is more tolerant of index mismatch. At the same imaging depth, a longer excitation wavelength with a larger index mismatch may lead to the same multiphoton signal and PSF degradation as a shorter excitation wavelength with a smaller index mismatch does.
(3) A longer excitation wavelength is more tolerant to larger imaging depth. For the same index mismatch, a longer excitation wavelength suffers from the same multiphoton signal and PSF degradation for a larger imaging depth, compared with shorter excitation wavelength.
(4) For the same excitation wavelength, the spherical aberration-induced multiphoton signal and PSF degradations are determined by the index mismatch, rather than by the specific immersion type.

Based on the above results, we suggest using longer excitation wavelength (e.g., choosing 1700-nm excitation) in MPM, if spherical aberration-induced signal and PSF degradations, as imaging depth increases, are to be avoided. However, we do note that the degradation of PSFs does not mean that at a certain imaging depth, the resolution with longer excitation wavelength is better than that with shorter excitation wavelength for the same imaging modality, measured in PSF. Avoiding excessive multiphoton signal degradation by resorting to longer wavelength is of vital importance for deep-tissue imaging, especially considering that so far the imaging depth is limited by signal depletion at the very deep regions of the tissue.

Conflict of Interest

The authors have declared no conflict of interest.

Acknowledgments

We acknowledge Prof. Ke Wang from Key Laboratory of Optoelectronic Devices and Systems of Ministry of Education and Guangdong Province, College of Optoelectronic Engineering, Shenzhen University for helpful discussions. This work was supported by the Science and Technology Innovation Commission of Shenzhen (JCYJ2016030715 0657874 and KQJSCX20160226194151) and the National Natural Science Foundation of China (No. 61475103).

References

1. W. Denk, J. H. Strickler, W. W. Webb, "Two-photon laser scanning fluorescence microscopy," *Science* **248**, 73–76 (1990).
2. M. E. J. Sheffield, D. A. Dombeck, "Calcium transient prevalence across the dendritic arbour predicts place field properties," *Nature* **517**, 200–204 (2015).
3. E. B. Brown, R. B. Campbell, Y. Tsuzuki, L. Xu, P. Carmeliet, D. Fukumura, R. K. Jain, "*In vivo* measurement of gene expression, angiogenesis and physiological function in tumors using multiphoton laser scanning microscopy," *Nat. Med.* **7**, 864–868 (2001).
4. W. R. Zipfel, R. M. Williams, R. Christie, A. Y. Nikitin, B. T. Hyman, W. W. Webb, "Live tissue intrinsic emission microscopy using multiphoton-excited native fluorescence and second harmonic generation," *Proc. Natl. Acad. Sci. USA* **100**, 7075–7080 (2003).
5. N. G. Horton, K. Wang, D. Kobat, C. G. Clark, F. W. Wise, C. B. Schaffer, C. Xu, "*In vivo* three-

photon microscopy of subcortical structures within an intact mouse brain," *Nat. Photonics* **7**, 205–209 (2013).

6. W. Wen, Y. Wang, H. Liu, K. Wang, P. Qiu, K. Wang, "Comparison of higher-order multiphoton signal generation and collection at the 1700-nm window based on transmittance measurement of objective lenses," *J. Biophotonics* **11**(1), e201700121 (2017).
7. S. Maiti, J. B. Shear, R. Williams, W. Zipfel, W. W. Webb, "Measuring serotonin distribution in live cells with three-photon excitation," *Science* **275**, 530–532 (1997).
8. L.-C. Cheng, N. G. Horton, K. Wang, S.-J. Chen, C. Xu, "Measurements of multiphoton action cross sections for multiphoton microscopy," *Biomed. Opt. Express* **5**, 3427–3433 (2014).
9. Y. Wang, K. Wang, W. Wen, P. Qiu, K. Wang, "Comparison of signal detection of GaAsP and GaAs PMTs for multiphoton microscopy at the 1700-nm window," *IEEE Photonics J.* **8**, 6803406 (2016).
10. R. M. Williams, W. R. Zipfel, W. W. Webb, "Interpreting second-harmonic generation images of Collagen I Fibrils," *Biophys. J.* **88**, 1377–1386 (2005).
11. D. Débarre, W. Supatto, A. M. Pena, A. Fabre, T. Tordjmann, L. Combettes, M. C. Schanne-Klein, E. Beaurepaire, "Imaging lipid bodies in cells and tissues using third-harmonic generation microscopy," *Nat. Methods* **3**, 47–53 (2005).
12. D. Kobat, M. E. Durst, N. Nishimura, A. W. Wong, C. B. Schaffer, C. Xu, "Deep tissue multiphoton microscopy using longer wavelength excitation," *Opt. Express* **17**, 13354–13364 (2009).
13. D. G. Ouzounov, T. Wang, M. Wang, D. D. Feng, N. G. Horton, J. C. Cruz-Hernández, Y. T. Cheng, J. Reimer, A. S. Tolias, N. Nishimura, C. Xu, "*In vivo* three-photon imaging of activity of GCaMP6-labeled neurons deep in intact mouse brain," *Nat. Methods* **14**, 388–390 (2017).
14. K. Wang, W. Wen, Y. Wang, K. Wang, J. He, J. Wang, P. Zhai, Y. Yang, P. Qiu, "Order-of-magnitude multiphoton signal enhancement based on characterization of absorption spectra of immersion oils at the 1700-nm window," *Opt. Express* **25**, 5909–5916 (2017).
15. Y. X. Wang, W. Wen, K. Wang, P. Zhai, P. Qiu, K. Wang, "Measurement of absorption spectrum of deuterium oxide (D_2O) and its application to signal enhancement in multiphoton microscopy at the 1700-nm window," *Appl. Phys. Lett.* **108**(2), 021112 (2016).
16. D. Day, M. Gu, "Effects of refractive index mismatch on three-dimensional optical data-storage density in a two-photo bleaching," *Appl. Opt.* **37**, 6299–6304 (1998).
17. C. Y. Dong, B. Yu, P. D. Kaplan, P. T. C. So, "Performance of high NA water and oil immersion objective in deep tissue, multiphoton microscopic imaging of excised human skin," *Microsc. Res. Tech.* **63**, 81–86 (2004).
18. A. N. Bashkatov, E. A. Genina, V. V. Tuchin, "Optical properties of skin, subcutaneous, and muscle tissues: A review," *J. Innov. Opt. Health Sci.* **4**, 9–38 (2011).
19. J. Binding, J. Ben Arous, J. F. Léger, S. Gigan, C. Boccara, L. Bourdieu, Brain refractive index measured *in vivo* with high-NA defocus-corrected full-field OCT and consequences for two-photon microscopy," *Opt. Express* **19**, 4833–4847 (2011).
20. P. A. Young, S. G. Clendenon, J. M. Byars, R. S. Decca, K. W. Dunn, "The effects of spherical aberration on multiphoton fluorescence excitation microscopy," *J. Microsc.* **242**, 157–165 (2011).
21. P. Torok, P. Varga, Z. Laczik, G. R. Booker, "Electromagnetic diffraction of light focused through a planar interface between materials of mismatched refractive indices: An integral representation," *J. Opt. Soc. Am. A* **12**, 325–332 (1995).